國立臺灣大學理學院心理學研究所

碩士論文

Graduate Institute of Psychology
College of Science
National Taiwan University

Master Thesis

色彩對比增益控制機制在整體圖形知覺扮演的角色

The role of color contrast gain control in global form perception

林易萱

Yih-Shiuan Lin

指導教授:陳建中 博士

Advisor: Chien-Chung Chen, Ph.D.

中華民國 105 年 7 月

July, 2016

doi:10.6342/NTU201600804

國立台灣大學理學院心理學研究所

論文口試委員會審定書

林易萱 先生所提論文 The Role of Color Contrast Gain Control in Global Form Perception

經本委員會審議，符合碩士學位標準，特此證明。

論文考試委員會

主席 黃碧烽

委員 黃碧烽 吳佳璘

黃從仁 陳建中

指導教授：陳建中

所主任：葉素玫

中華民國 105 年 6 月 27 日

doi:10.6342/NTU201600804

Acknowledgement

要如何寫致謝才不會落入老套的窠臼、又不至於虛偽浮誇呢？
答案就是「不可能吧！」
但我還是懷抱著雄心壯志
嘗試寫出一篇讓未來的某個日子裡回頭看會眼睛為之一亮的

謝詞

要感謝的人太多了
所以以下感謝的順序
純粹是自由聯想的結果
並不代表感謝的大小
或者對我的重要性

老闆 吻
感謝你總是讓我插隊問問題，即使你一定覺得我超級吵
感恩你放任我到處亂入實驗，最後還要你幫我收拾善後
感激你教會我哪些事情重要，哪些又是煩瑣無謂的掙扎
實驗室的夥伴 們
感念你們忍受我的魔音穿腦，我一興奮起來就分貝爆表
感動各位願意當我的受試者，沒有你們我究竟該怎麼辦
感佩大家都活力充沛地交流，每天享受腦力激盪的快感
最愛的午餐夥伴 們
如果沒有你們每天揪團吃飯，我這兩年一定是相當淒涼
如果沒有大夥一起同仇敵愾，自命不凡的驕傲如何發洩
如果沒有群情無條件的支持，這一路走來不會如此順遂
芝玉路的家人 們
好想當面告訴你們但我害羞，二十四年來每天都很愛你
好想讓時間不會滴答向前走，於是我們就能永遠當家人
好想要全世界都知道並明白，甚麼叫做無怨無悔的後盾
那些沒法細數的人 們
就算現在沒有一一列舉出來，也不代表你們不值得感謝
就當做我的腦容量非常有限，沒有一一記住你們的名字
就相信我真誠打從心理感謝，當初與你們相遇的一瞬間

doi:10.6342/NTU201600804

新詩最棒的地方

就是

不管你寫的再怎麼爛

別人看了

都會說

啊

這就是藝術

學術這條路

真的不好走

人生這條路

根本更難走

可是你知道嗎？

嘿

我成功從念了六年的台大畢業了

所以

未來的你

得到這麼多幫助給了這麼多感謝

一定可以走得　更長　更久 更好 更遠

All that is gold does not glitter,
Not all those who wander are lost;
The old that is strong does not wither,
Deep roots are not reached by the frost.

-J.R.R Tolkien

I'm not crazy. My reality is just different from yours.

-Cheshire Cat

doi:10.6342/NTU201600804

摘要

葛拉斯(Glass)圖形是由隨機散佈的「雙點（dipole）」部件所組成，而這些雙點之間的排列遵照特定的幾何規則，不同的規則將決定該圖形的整體知覺。知覺一個葛拉斯圖形仰賴兩階段的處理機制，局部處理—將兩個點組合成雙點部件—以及整體處理—將這些局部的雙點部件整合成整體的圖形。有別於傳統的葛拉斯圖形，在我們的研究中我們使用局部由「三點（tripole）」部件組成的葛拉斯圖形，以之研究色彩對比（color contrast）對於人類群聚視知覺（visual grouping）的影響。每個三點部件包含一個定錨點（anchor dot）與兩個周邊點（context dot），將定錨點與其中一個周邊點整合則葛拉斯圖形整體看起來會呈現為一個逆時針螺旋，與另一個周邊點整合則會看成順時針螺旋。在我們的色彩操弄中，每個三點葛拉斯圖形中的所有點色調（hue）一致，只有色彩對比有所不同。我們使用四種色調的刺激，對比根據+/-(L-M)以及+/-S 主軸軸線變化。實驗參與者必須在看完每個三點葛拉斯圖形之後判斷該圖形是順時針還是逆時針的螺旋並按下相對應的反應按鍵。結果發現判斷圖形為順時針或逆時針螺旋的機率會隨著其中一個周邊點的色彩對比上升，直到超過特定的對比值後該機率又會下降；而整體的機率又會隨著另外一個周邊點的對比上升而下降。這樣

doi:10.6342/NTU201600804

的結果無法用過去提出的理論模型來解釋，而必須使用我們提出的「除法抑制模型(divisive inhibition model)」才能解釋資料變異。本研究得到的結果與之前操弄明暗對比(luminance contrast)類似，都有呈現倒U(inverted-U)的趨勢，相異之處在於色彩對比模型中的抑制部件較明暗對比來的弱。

關鍵字：葛拉斯圖形 、色彩對比、對比增益控制、知覺群聚效應、物體辨認。

doi:10.6342/NTU201600804

The Role of Color Contrast Gain Control in Global Form Perception

Yih-Shiuan Lin

Abstract

A Glass pattern consists of randomly distributed dot pairs, or dipoles, whose orientation is determined by a geometric transform, which defines the global percept perceived by an observer. The perception of Glass patterns involves a local process that associates dot pairs into dipoles and a global process that groups the dipoles into a global structure. In the present study, we used a variant of Glass patterns, which was composed of randomly distributed tripoles instead of dipoles, to estimate the influence of color contrast on perceptual grouping. Each tripole contained an anchor dot and two context dots. Grouping the anchor dot with one of the context dot would result in a global percept of a clockwise (CW) spiral while grouping with the other dot, a counterclockwise (CCW) spiral. All dots in each pattern were modulated in the same color direction but different contrasts. Four types of patterns were involved, namely modulating in +/-(L-M), and +/-S cardinal directions. The observers were to

doi:10.6342/NTU201600804

determine whether the spiral in each trial was CW or CCW. The probability of a context dot being grouped with the anchoring dot increased along with its color contrast to certain level before the probability started to drop. Our result cannot be explained by the existing models for perceptual grouping but a divisive inhibition model. The isoluminance contrast result observed is similar to the inverted U-shaped function for luminance contrast result previously reported (by us); except that color contrast model comprises a weaker self-inhibition component.

Keywords: Glass pattern, color contrast, contrast gain control, perceptual grouping, object recognition.

doi:10.6342/NTU201600804

Table of Contents

doi:10.6342/NTU201600804

doi:10.6342/NTU201600804

List of Tables

doi:10.6342/NTU201600804

List of Figures

doi:10.6342/NTU201600804

doi:10.6342/NTU201600804

doi:10.6342/NTU201600804

Introduction

Humans are visual animals. To survive in nature, one needs to spot camouflaged predators, locate suitable food in complicated backgrounds, and familiarize a new environment as soon as possible. Thus, it makes processing natural scenes a vital task in our lives.

One important step of scene perception is to parse a scene into meaningful shapes and objects. Recognizing objects requires a hierarchical process throughout the brain (Felleman & Van Essen, 1991; Van Essen, Anderson, & Felleman, 1992), from low level visual areas to high level ones, from detailed and local information to general and global representations.

Along this object processing hierarchy, V1, or primary visual cortex, is the first cortical area that receives retinal signals via lateral geniculate nucleus (LGN). V1 neurons possess relatively small receptive fields (RFs) that tune to elementary properties of object such as orientation, edges and contours (Hubel & Wiesel, 1968). Immediately adjacent to V1, V2 has neurons with RFs larger than primary visual cortex. Neurophysiological evidence has shown that these V2 RFs tune to

doi:10.6342/NTU201600804

combination of orientation (Anzai, Peng, & Van Essen, 2007) and angles embedded within contours (Hegdé & Van Essen, 2000; Ito & Komatsu, 2004), suggesting that from V2 the visual system has begun to extract form and shape information out of local elements. The information is then sent to V4, where more complicated shape information is encoded. Gallant, Braun, and Van Essen (1993) demonstrated that neurons in macaque V4 showed selective response to polar, hyperbolic and vertical or horizontal gratings. Pasupathy and Connor (2002) discovered that population coding in macaque V4 can explain how neurons process complex forms, supporting that V4 is responsible for processing curving shapes. These intermediate form information processed by striate cortex will then be sent to the highest visual areas, inferotemporal (IT) cortex and lateral occipital cortex (LOC). The neurons in these high-level regions respond to complicated shapes and forms such as faces (Goodale & Milner, 1992; Tanaka, 1996).

Through feeding forward and feedback processing between these cortical areas mentioned above, the visual system forms the final representation of objects in the outside world. This processing stream occurs mostly in the ventral part of the

doi:10.6342/NTU201600804

cerebral cortex; therefore, it is considered as the ventral pathway of visual system (Mishkin, Ungerleider, & Macko, 1983; Riesenhuber & Poggio, 1999). As the information processing progresses, the visual system gradually relieves the neurons from encoding information within a particular physical area. One example is the enlargement of RFs in higher visual area, proving that less neurons cover the same retinal region. The other example is the progressing extraction of abstract properties from stimuli, indicating that the visual system is using less cells to represent an object in higher level regions (for a review of object processing in the ventral stream, see Wilson and Wilkinson, 2015).

The consequence of this hierarchical processing, at the behavior level, is reflected in perceptual grouping, the integration of local basic units into global forms. Examples are identifying contours and boundaries by linking adjacent edges and segregating different objects by organizing similar elements into uniform surfaces. Gestalt principles like proximity, similarity, and figure-ground segregation have been frequently used to explain how our visual system integrates basic elements into objects (Metzger, Spillmann, Lehar, Stromeyer, & Wertheimer, 2006).

doi:10.6342/NTU201600804

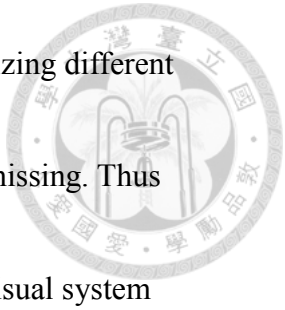

Whilst Gestalt theory provides a good framework of categorizing different types of grouping, information about the underlying mechanism is missing. Thus Gestalt theory cannot answer questions such as when and why the visual system chooses one rule over another, and how the visual system possesses these fundamental rules at the first place. To understand how the visual system achieves the final groupings, a systematic investigation of how the manipulation of local element properties affects the global percept is necessary. By doing so, we can then construct a bottom-up model describing the grouping mechanisms of how the visual system processes visual inputs (physical stimuli) and produces perceptual outputs (grouping percept).

Glass patterns have been widely used to gain better understanding of the mechanisms of perceptual grouping. A Glass pattern (Glass, 1969; Glass & Perez, 1973) consists of two random dot patterns superimposed upon each other conforming a geometric transform (see Figure 1). The merit of Glass pattern is that its perception requires at least two stages of grouping processing. The first is the local processing, one needs to group local two dots together to perceive dipoles. Second is the global

doi:10.6342/NTU201600804

processing, these dipoles must be grouped into a global structure to achieve the global form percept. Taking the advantage of the characteristic of processing Glass patterns, we investigated how changing the local element properties of Glass patterns affects the global grouping percept.

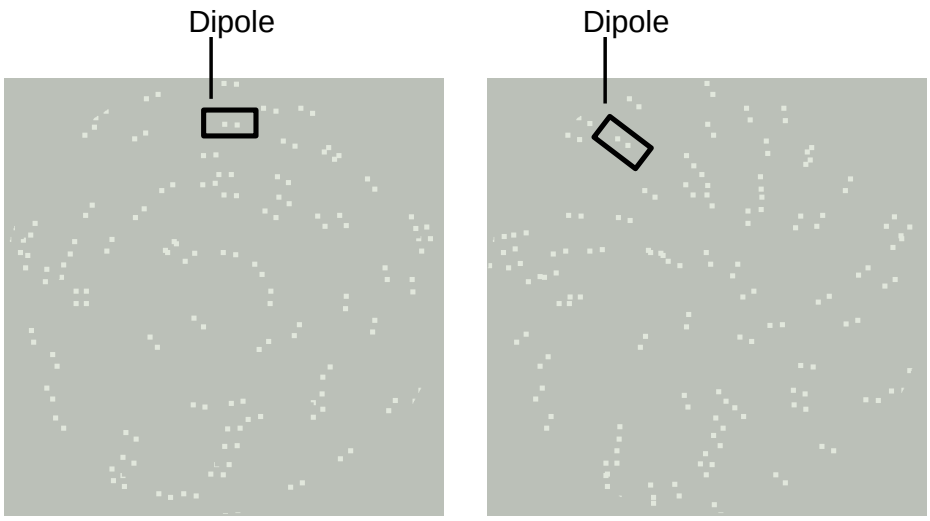

Figure 1. Demonstration of traditional Glass patterns comprised of local dipoles (two-dot pairs circled in the figure). Left pattern is perceived as a concentric global pattern while the right one a spiral pattern.

Many have manipulated the components and properties of dipoles, or the local units, to observe how visual system creates linkage between them. Some changed the distance between two dots to measure the spatial frequency tuning (Dakin, 1997; Dakin & Bex, 2001), others manipulated the shape (Stevens, 1981), orientation (Wilson, Wilkinson, & Asaad, 1997), luminance contrast (Badcock, Clifford, & Khuu,

doi:10.6342/NTU201600804

2005; Chen, 2006; Wilson, Switkes, & De Valois, 2004), and chromaticity (Cardinal & Kiper, 2003; Mandelli & Kiper, 2005; Wilson & Switkes, 2005) of local elements. These research provided insight into circumstances of which human may detect the global form most effectively; thus, shed light on the tuning functions of the visual system toward these visual cues.

However, the paradigms employed by these studies offer little information regarding to the consequences of simultaneous presentation of multiple global forms. Chen (2009) used masking paradigm to tackle the interference between different types of Glass patterns. In the experiments, Chen used concentric and radial Glass patterns as targets and measured the detection thresholds of these targets masked by various maskers (random noise as well as vertical, plaid, radial, concentric, or spiral Glass patterns) at different density levels. Chen reported that the TvD (threshold vs. density of the masker) functions of targets changed with masker types and, thus, proposed curvature selectivity in the global form processing of Glass pattern perception.

To further examine the competition between the global forms in Glass pattern perception, we designed a variant of Glass pattern (illustrated in Figure 2) that locally

doi:10.6342/NTU201600804

contains three-dot pairs, or tripoles, instead of dipoles (see **Method** for detailed description of how we generated tripole Glass patterns, or tGPs). For this kind of configuration, locally, one can perceive three possible dipoles, competing with each other. The three possible configurations are indicated by the colored ovals in the right panel in Figure 2.

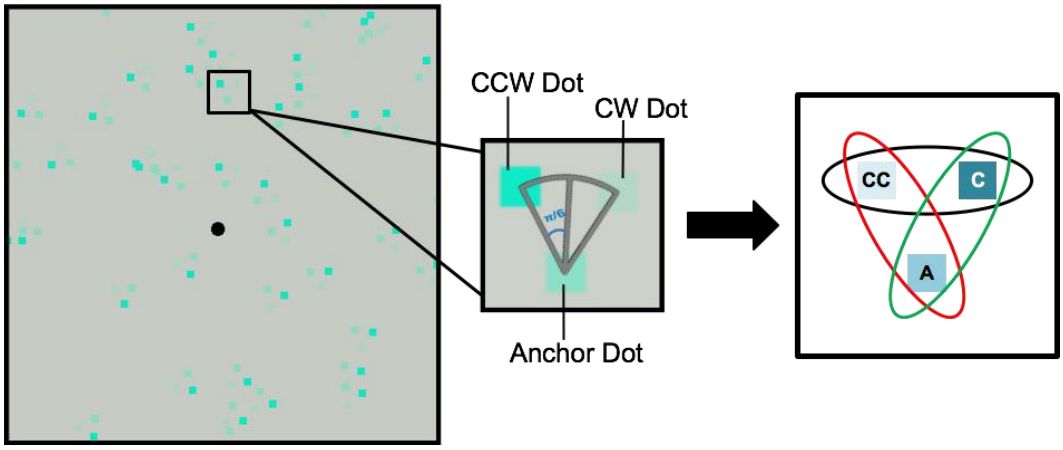

Figure 2. An illustration of our stimulus. This version of Glass pattern is composed of multiple local "tripoles". Locally, a tripole (the zooming-in image in the middle panel) comprises three equal-size dots positioned in equal distance. As shown by the panel on the right, within each tripole, the anchor dot (the square with an "**A**" on it) can be grouped with CCW dot (the square denoted "**CC**"), shown as the red oval, or CW dot (the square denoted "**C**"), the green oval. The former will result in a global percept of a counter-clockwise (CCW) spiral whilst a clockwise (CW) spiral resulting from the later. The example tripole Glass pattern presented on the left is most likely to be perceived as a counter-clockwise spiral (see text for detailed description). Although there can be yet another grouping result (CCW dot grouped with CW dot forming a concentric global form, as indicated by the black oval), we found that it had no significant effect when we fitted our model to the data collected (elaborated in **Discussion** section).

doi:10.6342/NTU201600804

Previously, we examined the effect of luminance contrast in tGP perception (Cho, 2015). We presented tGPs on an isochromatic (or gray-scale) plane while manipulating the luminance contrast of the anchor dot and the two context dots (CCW dot and CW dot). Our results showed that the probability of participant judging the tGP as a clockwise spiral first increased with the contrast level of CW dot then decreased once the contrast level passed a certain point. This inverted-U trend was modulated by the contrast of CCW dot for the overall probability was reduced as the contrast of CCW dot increased.

The results cannot be fully explained by the existing models in the literature. Prazdny (1984) reported a series of experiments in which two or more organizations of Glass patterns (with various feature domains) were superimposed. Through recording the global percept of the observer, Prazdny was able to underpin the features that outperformed the others and to determine the global processing. According to Prazdny, features that were stronger in spatial and energy domain determined which global form participants perceived. In this case, energy was defined as the product of the size and the magnitude of contrast, regardless of polarity, of the

doi:10.6342/NTU201600804

features used. This energy model partially explains our data where the grouping probability increased as the CW dot contrast increased (stronger energy) but fails to explain the reduction of grouping strength once the probability goes beyond the peak, which results in an inverted-U shape. On the other hand, Earle (1999) reported that luminance contrast determined the grouping of two dots within a three-dot local pair in similar fashion. The results showed that a low contrast dot was more likely to be paired with another low contrast dot than with a high contrast dot to construct a global vertical or horizontal pattern. Similarly, Wilson et al. (2004) found that contrast difference between two dots in one dipole reduced the probability that they would be grouped together. These results are taken as supporting evidence for token-matching theory, which proposes that the more similar the elements, the more likely they will be grouped together. Based on the token-matching theory, it is predicted that the highest grouping probability happens when the contrast of one of the context dot matches the contrast of the anchor dot. However, that was not the cases of the current study, the findings revealed that the peak probabilities did not occurred when anchor dot and CW dot were of the same contrast level.

doi:10.6342/NTU201600804

A divisive inhibition model (Chen, 2009; Chen, Foley, & Brainard, 2000), on the contrary, can successfully explain both aspects of our results (see **Discussion** for model details). In fact, being able to fit the divisive inhibition model to the data implies the involvement of a contrast gain control mechanism in grouping percept of Glass patterns.

Despite previous studies suggest that luminance and color contrasts contribute differently in vision, the role of color contrast in visual grouping has been overlooked. First of all, spatial frequency tuning has been found to be lower for chromatic than achromatic gratings in psychophysics (Losada & Mullen, 1994; Mullen, 1985), electrophysiological (Tobimatsu, Tomoda, & Kato, 1995), and neurophysiological experiments (Johnson, Hawken, & Shapley, 2001; Kaplan, Shapley, & Purpura, 1988; Thorell, de Valois, & Albrecht, 1984). In addition, although color and luminance stimuli both showed selectivity to orientation and spatial frequency, contrast thresholds showed little elevation when using luminance grating to adapt for chromatic gratings, or vice versa (Bradley, Switkes, & De Valois, 1988). This evidence suggests that chromaticity and luminance are processed by different neural

doi:10.6342/NTU201600804

mechanisms. We expected to find different results of competition between grouping patterns in tripole Glass patterns when chromatic stimuli instead of achromatic ones were used. Also, since both contrasts used in the present study and Cho (2015) were cone contrast, we could directly compare the results of Cho (2015) and that of the present study. If we can apply the same contrast gain control model to these two different kinds of contrast (luminance and color) to explain the local to global grouping of Glass pattern, then we can conclude that the gain control mechanism is a common mechanism underlying visual grouping.

To sum up, we address two issues in the present study. First, we want to know whether there is any competition between global grouping outcomes presented simultaneously by using tripole Glass patterns as stimuli. This question cannot be answered by past research because that most studies investigating visual grouping with Glass patterns used stimuli containing only one possible global form, sometimes embedded in random noise (Badcock et al., 2005; Cardinal & Kiper, 2003; Chen, 2006; Dakin, 1997; Dakin & Bex, 2001; Mandelli & Kiper, 2005; Wilson et al., 1997; Wilson & Switkes, 2005; Wilson et al., 2004). Even though Earle (1999) did use

doi:10.6342/NTU201600804

tripole patterns similar to ours, he failed to systematically vary different contrast levels of competing dot pairs. Second, we will explore the role color contrast plays in perceptual grouping. Though past researches have used chromatic Glass patterns (Cardinal & Kiper, 2003; Mandelli & Kiper, 2005; Wilson & Switkes, 2005), they focused more on perceptual tunings by measuring detection thresholds of patterns varying in chromaticity instead of addressing competition between global forms.

doi:10.6342/NTU201600804

Method

Participants

Three observers participated in this experiment, including the author (LYS) and two other participants who were naïve to the purpose of this study. All the observers had normal (20/20) or corrected-to-normal visual acuity. The study was approved by the Institutional Review Board (IRB) of National Taiwan University Hospital. Written consent was obtained from each observer before the experiment.

Apparatus

We used a 24-inch EIZO LCD monitor (FlexScan SX2462W) for stimuli presentation. A Macintosh computer through an ATI Radeon HD 4870 graphics board, providing 10-bit digital-to-analog converter depth, controlled the monitor. The refresh rate of the LCD monitor was 86 Hz. The luminance and chromaticity of the monitor were calibrated with a Photo Research PR655 radiometer. The display showed a mean luminance of 69.6125 cd/m^2 and mean chromaticity at (0.3354, 0.3342) in CIE 1931-xy coordinates. The viewing distance between observer and the center of the monitor was set such that each pixel extended 1 min of visual angle.

doi:10.6342/NTU201600804

Stimuli

Different from the traditional Glass pattern, which consisted of two-dot pair (dipole) locally, a variant Glass pattern composed of three-dot pairs was used to form "tripoles", as shown in Figure 2. To generate a tripole Glass pattern (tGP), we first drew randomly distribute square dots (7' x 7' visual angle) in the stimulus field as anchor dots (illustrated as the square denoted "**A**"). We chose relatively larger dots than used in previous isochromatic experiments (Chen, 2009; Li & Chen, 2011) to accommodate the lower spatial frequency tuning for chromatic stimuli and to avoid chromatic aberration. Context dots (CCW dot and CW dot, depicted by squares with "**CC**" and "**C**" in Figure 2) that had the same size as the anchor dot were placed on either side of the radial line passed through the anchor dot. The line that passed through a context dot and the anchor dot intercepted the radial line with an angle $\boldsymbol{\pi}/6$. Thus, three dots in a tripole formed the vortices of an equilateral triangle, with the anchor dot pointing toward the center of the display. The distance between two dot centers in a tripole was 17'.

The global structure of our tripole Glass patterns were derived from

doi:10.6342/NTU201600804

Archimedean spirals, which was defined as Eq. 1, where r and θ were the radiance and azimuth of a dot, a defined the phase of the spiral that passed the anchoring dot, and b determined the curvature of the spiral.

$$r = a + b\theta \quad (1)$$

Since dot density was found not to have a large effect on thresholds detection (Wilson & Wilkinson, 1998), we chose a low dot density of 4% so that tripoles were unlikely to overlap with each other. The overall size of global Glass patterns was 10 degrees visual angle.

The chromaticity were defined in polar coordinates of a cone contrast space (Derrington, Krauskopf, & Lennie, 1984; MacLeod & Boynton, 1979), in which elevation represented the luminance, azimuth the hue, and distance to origin the contrast. Here we chose four colors, along with L-M modulation and S modulation, which were red (azimuth angles 0°), green (180°), blue (90°), and yellow (270°). The chromaticity of each dot was defined by a contrast vector with three contrast values, $C = [C_L, C_M, C_S]$, C_L being the L-cone contrast, C_M the M-cone contrast and C_S the S-cone contrast. The L-cone contrast, C_L, was defined as $\Delta L/L_0$, where L_0 representing

doi:10.6342/NTU201600804

the L-cone excitation produced by the background and ΔL the increments or decrements of the L-cone excitation produced by the dot. The M-cone and S-cone contrasts, C_M and C_S, were defined similarly. Cone excitations were estimated as the product of the power spectral distribution of the input light and the spectral sensitivity functions of each cone (Stockman & Sharpe, 2000). Eventually each contrast vector was composed of a scalar value for contrast and a normalized cone contrast vector, $C / ||C||$, where $||C||$ denotes the length of the vector C. In the present study, the normalized cone contrast vectors used were [0.416, -0.909, 0] for red, [-0.416, 0.909, 0] for green, [0, 0, 1] for blue, and [0, 0, -1] for yellow[1]. Note that the normalized cone contrast vectors for isoluminant stimuli were all orthogonal to the CIE 2007 luminous efficiency function V_λ(CIE, 2007), which corresponded to the normalized vector [0.853, 0.522, 0]. The final contrast of each dot was defined as $C = (C_L^2 + C_M^2 + C_S^2)^{0.5}/3^{0.5}$, proportional to the square root of the cone contrast energy and varied between 0 and 1. Contrast was expressed in dB, which equaled $20*\log_{10}C$, ranged from -∞ to 0.

[1] For a comparison, the contrast vectors used in Cho (2015) was [0.577, 0.577, 0.577] and [-0.577, -0.577, -0.577] for white and black respectively,

doi:10.6342/NTU201600804

For each tGP presented, all dots belonged to one of the four hues mentioned above. Since human L and M cones have higher input sensitivity than S cones and easily become saturated under high contrast, we chose contrast levels based on the detection thresholds of these colors in a way that contrasts covered from near threshold level to saturating level. See **Appendix** for how we estimated the thresholds. Thus, for red and green, contrasts of context dots were ranged from -35 dB to -12 dB and being of either -30 dB or -18 dB for anchor dots. As for blue and yellow, context dots contrasts were within a range between -13 dB to -1 dB with the anchor dots always kept at -7 dB. The luminance of all dots matched that of the background (mean luminance) so that luminance contrast would not contaminate the effect of chromatic contrast.

Procedure

A 2AFC (two-alternative forced-choice) paradigm experiment was developed. The tripole Glass patterns of different hue were organized into four sessions, each containing at least 10 runs. In every run, all combinations of context dots contrast were randomly presented four times. Thus, overall, there were 40 measurements for

doi:10.6342/NTU201600804

each combination.

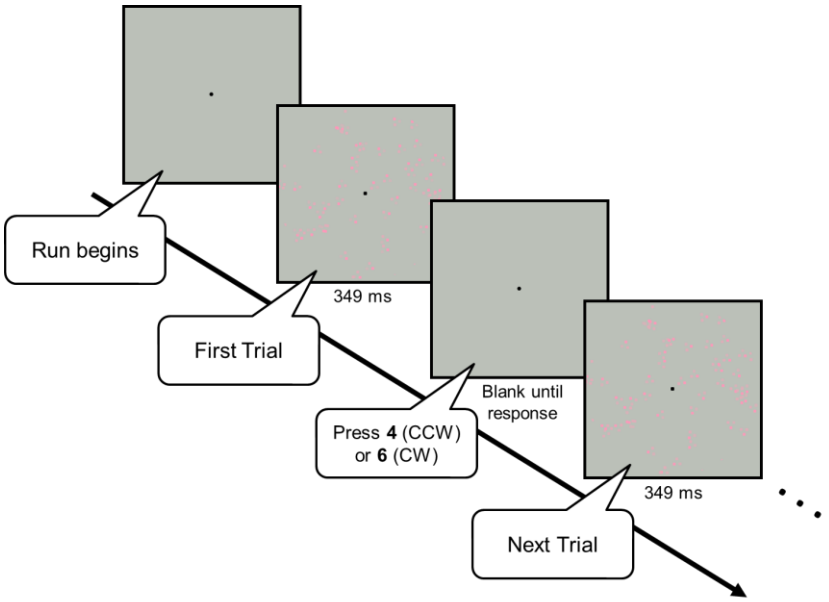

Figure 3. A schematic procedure of the 2AFC experiment. Observers were to press key 4 to indicate they saw a counter-clockwise (CCW) spiral, key 6 a clockwise (CW) spiral.

In each trial, after an auditory cue indicating the start of a new trial, one tGP was presented on the monitor with duration of 349 ms, together with a fixation point in the center. We chose a relatively long duration due to the exiting knowledge that chromatic stimuli were processed slower than the luminance ones. Participants were to decide whether the pattern was a clockwise (CW) spiral or a counter-clockwise (CCW) one by pressing the corresponding key. The next trial would not start until response was received (see Figure 3 for the schematic procedure). We recorded the probability of the observer reporting CW under each contrast combination.

doi:10.6342/NTU201600804

Results

Red and Green (L-M modulation)

We first tested red and green tGPs with -18 dB anchor contrast and two context dots ranged from -21 to -12 dB, labeled high contrast anchor condition. By presenting dots with contrast levels way above red/green threshold (about -33 dB), we could reassure that the participants had no difficulty seeing the stimuli.

Figure 4 shows results of high anchor condition for all three participants. In each panel, the y-axis denotes probability judging red and green tGP as a clockwise spiral, with x-axis showing the contrast level of CW dot and y-axis the judging probability. Each row contains data of one observer, with initials labeled alongside. Filled colored circles are the original data points measured in our 2AFC experiments, while colored curves being the fitting results of our divisive inhibition model mentioned before (the results of model fitting are listed in the **Discussion** part), The contrast of CCW dot is the same in each curve while contrast of CW dot changes from low to high, left to right. The dashed vertical lines in each panel indicate contrast level of the anchor dot, so data points where these dashed lines pass through are results when CW dot and

doi:10.6342/NTU201600804

anchor dot had the same contrast level.

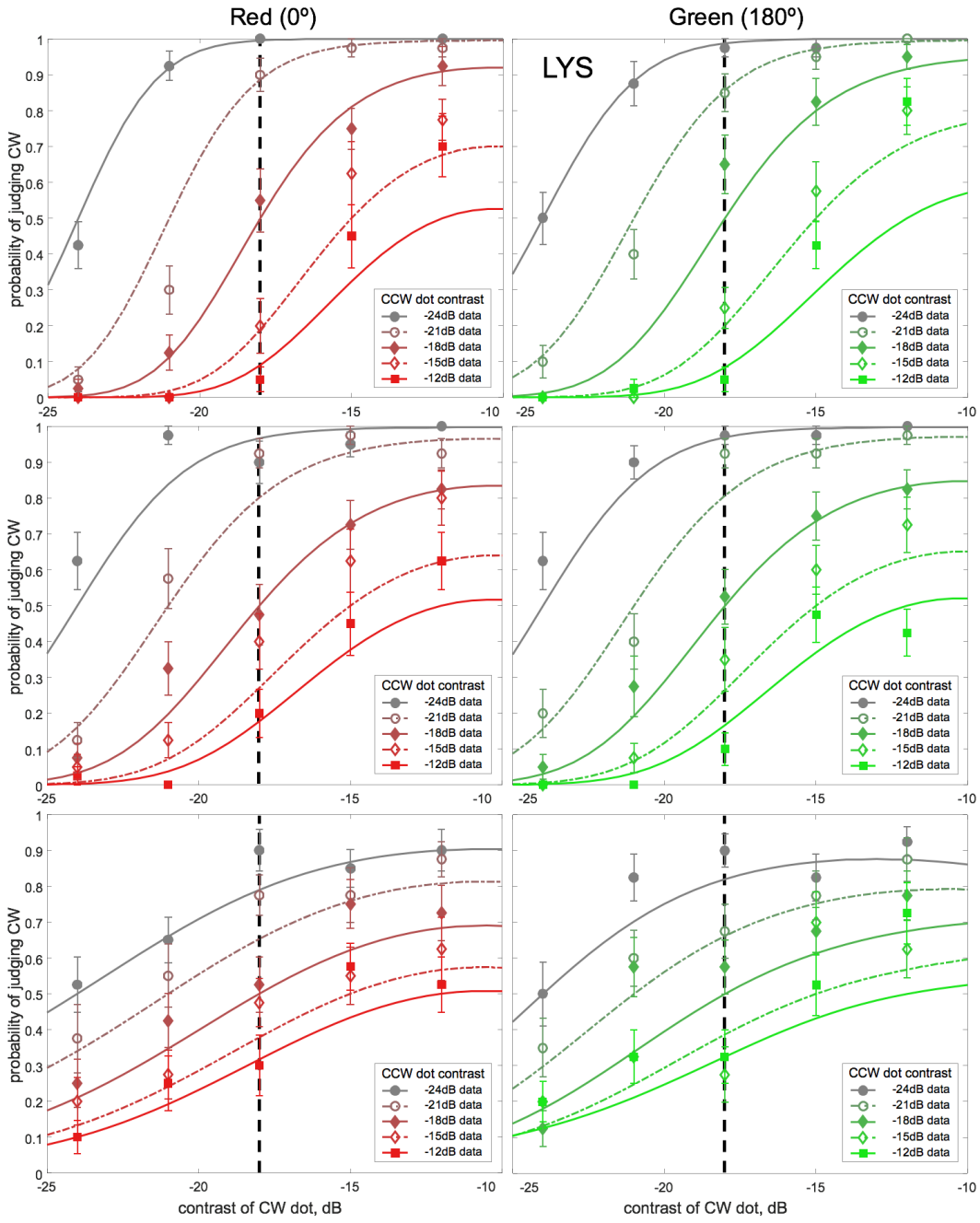

Figure 4. Results of red and green condition with -18 dB anchor dot. Figure here shows probability of three participants in judging tGPs as CW spiral across different CCW dot and CW dot contrasts. The circles, diamonds and squares demonstrate the raw data points, while the curves show the fitting results of our model. Dashed lines indicate the contrast level of the anchor dot.

doi:10.6342/NTU201600804

Results showed that as the contrast of CW dot began to rise, the participants had a higher tendency to report the tGP as a CW spiral. However, the probability stopped increasing after a critical point and stayed constant afterwards. In addition, the probability of judging CW spiral decreased as the contrast level of CCW dot (CCW dot) increased.

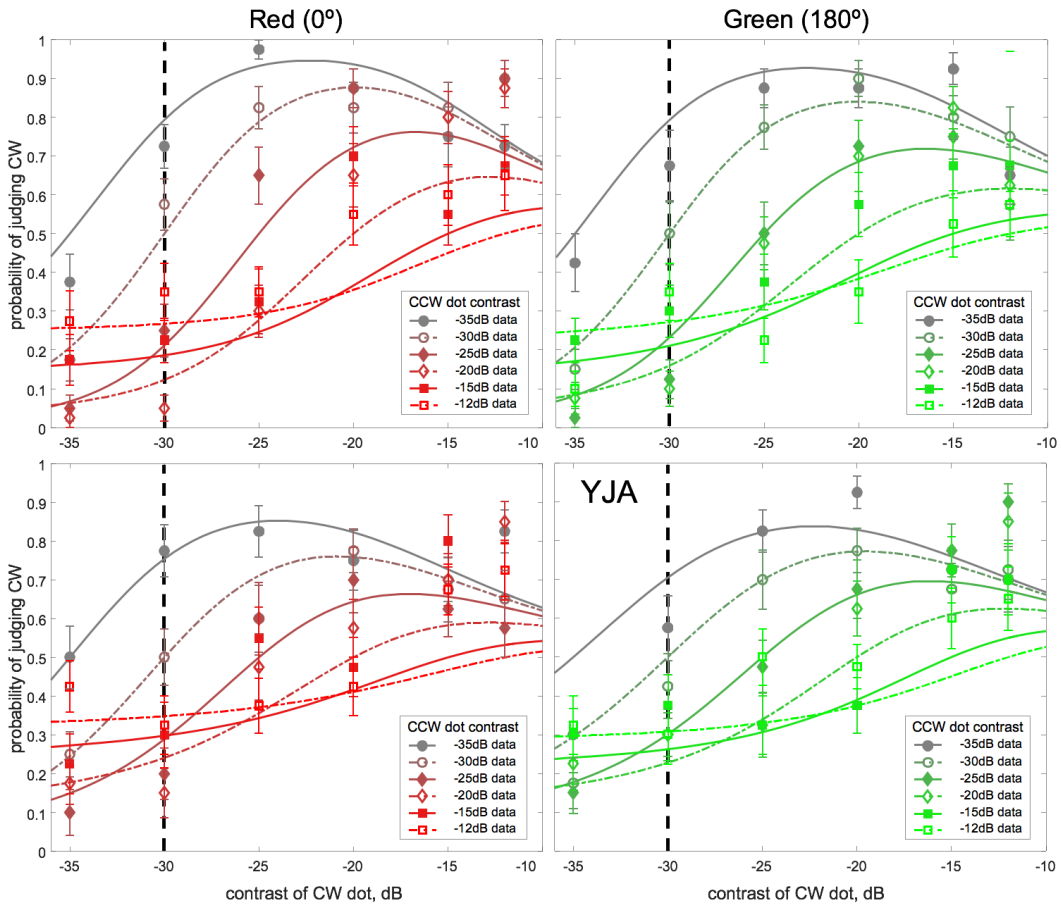

Figure 5. Results of red and green condition with -30 dB anchor dot. Figure presents robability of two participants making CW judgement across different CCW dot and CW dot contrasts. The circles, diamonds and squares represent the raw data points across different contrast levels, while the curves show the fitting results of our model. Dashed lines indicate the contrast level of the anchor dot.

doi:10.6342/NTU201600804

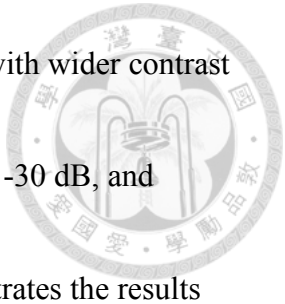

Next, to examine the competition between competing dipoles with wider contrast difference between dots, we used an anchor dot with lower contrast, -30 dB, and context dots of contrastranged from -35 to -12 dB. Figure 5 demonstrates the results of low anchor condition. The results were similar to that of high contrast anchor condition except for one major difference: the reducing of grouping probability after the contrast level of CW dot (CW dot) passed a certain level, leading to an inverted-U shape curve[2].

Blue and yellow (S modulation)

For blue and yellow tGPs, since the contrast range used in red/green low anchor condition could not be reached, we only tested them with high anchor contrast -7 dB, with context dots ranged from -13 to -1 dB.

The results of blue and yellow colors are presented in Figure 6. Two similar trends were found. First, the probability of judging CW increased with contrast of CW dot. Second, the overall probability decreased as the contrast of CCW dot.

[2] Also note that only two of the observers completed experiments in low contrast condition for observer YWH reported failure to perceive most of the dots with low contrast values.

doi:10.6342/NTU201600804

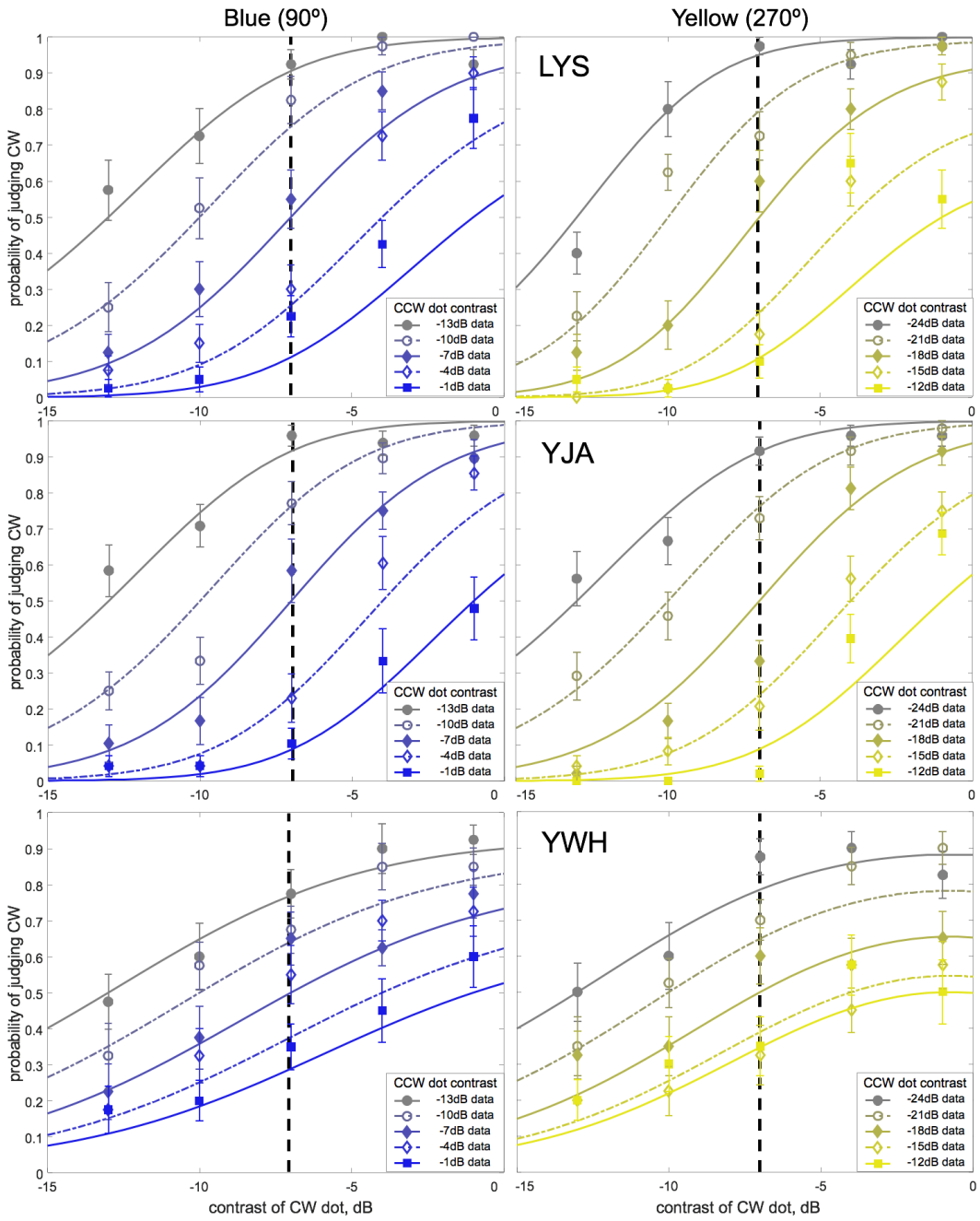

Figure 6. Results of blue and yellow condition with -7 dB anchor dot. Figure presents probability of two participants making CW judgement across different CCW dot and CW dot contrasts. The circles, diamonds and squares demonstrate the raw data points, while the curves show the fitting results of our model. Dashed lines indicate the contrast level of the anchor dot.

doi:10.6342/NTU201600804

doi:10.6342/NTU201600804

Discussion

We aimed to answer two questions in the present research. First is whether there is a competition between co-existing grouping outcomes. Second is what role does color play in Glass pattern perception.

To address the first issue, we created a tripole Glass pattern with multiple dipoles presented within each local tripole. Clear competition between possible grouping outcomes within one Glass pattern was observed. The global percept conformed to one of the dipoles (e.g. clockwise dipole) was affected by the contrast of the other dipole (e.g. counter-clockwise dipole). By manipulating both context dots across various color contrasts, we showed a clear inhibition effect of one dot pair to the other. That is, dot probability of participants judging global percept based on one dot pair decreased as the contrast of the other dot pair (others-inhibition). In addition, for red and green stimuli, as the contrast of one dot pair increased, the judging probability first increased then decreased after a certain contrast level (self-inhibition).

As for the second issue, we found that, for color stimuli, the self- and others-

doi:10.6342/NTU201600804

inhibition interacted with each other while competing dipoles can be explained by a contrast gain control model. The results of color were similar to that of luminance contrast, suggesting a universal process for all cone contrasts.

In the next section the model used in our study is introduced, and the results with the variation and relationship between model parameters and components are explained. In addition, we compare the current fitting outcomes with those reported by Cho (2015) to examine whether there is difference in the parameters between isoluminance and isochromatic results.

Model

We fitted a divisive inhibition model, which describes a contrast gain control mechanism, to our data. In our model, we first calculate the responses towards all possible dipoles in one local tripole, which are counter-clockwise (CCW) dipole, clockwise (CW) dipole and irrelevant dipole[3], demonstrated in the schematic diagram in Figure 7. The neural activation of one dipole is affected by the area the two dots cast on the receptive field targeting the dipole. Thus the activation toward one dipole

[3] This third dipole is named irrelevant because we found no difference in fitting outcomes whether we involved its contrast as model input or not (explained in the following paragraphs where we discuss model parameters). Thus we consider its effect to be null or minimum in our case.

doi:10.6342/NTU201600804

is determined by both the spatial factor (size of the dots) and the contrast factor (in our case, color contrast) and each factor decides the magnitude of activation variation when changing the other. Since the spatial factor is fixed in the current study (dot size was the same for all dots) while the contrast factor changes with the contrast level of these dots, the spatial factor independent of contrast can be seen as the sensitivity of neurons towards contrast change of the dipole. That is, the activation we had measured was the result of dipole contrast multiplies contrast sensitivity. So in our model both the excitatory and inhibitory activations are defined as the sensitivity times the color contrast.

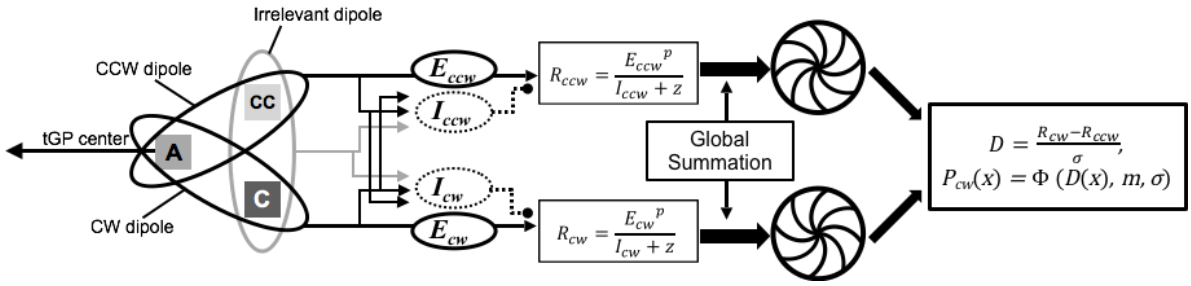

Figure 7. This figure illustrates the model used in the current study. See text in **Introduction** and **Discussion** for detailed description.

Take the response to CW dipole as an example. In Eq. 2, R_{cw}, is composed of an excitatory component in the numerator (E_{cw}), and an inhibitory component (I_{cw}) as well as a normalizing parameter (z) in the denominator. The E_{cw} is determined by

doi:10.6342/NTU201600804

contrast of CW dipole, C_{cw} (here, the sum of contrast values from both dots within the CW dipole) and the sensitivity toward CW dipole, Se_{cw}. I_{cw} is defined as the sum of C_{cw} and the contrasts of the other dipoles, C_{ccw} and C_{irre} after timing their sensitivity coefficients, Si_t, Si_1, and Si_2, respectively (Eq. 3). The subscript *t* indicates that the dipole being discussed is the "target dipole" while *1* and *2* mean the sensitivity toward the competing dipole (here, CCW dipole) and the sensitivity toward the irrelevant dipole respectively.

$$R_{cw} = \frac{{E_{cw}}^p}{I_{cw} + z} \tag{2}$$

$$E_{cw} = Se_{cw} * C_{cw}, \; I_{\mathrm{cw}} = (Si_t * \mathrm{C_{cw}})^q + (Si_1 * C_{ccw})^q + (Si_2 * C_{irre})^q \tag{3}$$

Then we assumed a linear global summation to integrate these local responses into global response. That is, the global response is the local response times a constant[4] determined by the total number of tripoles in one tGP. The final decision is determined by the response to CW dipole subtracting the response to CCW dipole, denoted D_{cw} in Eq. 4. We determine the judging probability by finding the probability value corresponding to this difference in a Gaussian cumulative distribution function

[4] For the value of this constant does not affect the model fitting result, we do not express it in the equation and will not discuss it further.

doi:10.6342/NTU201600804

(cdf), Φ, with mean (m) set at 0 and variance (σ) at 1 (Eq. 5).

$$D_{cw} = \frac{R_{cw} - R_{ccw}}{\sigma} \quad (4)$$

$$P_{cw}(D_{cw}) = \Phi\,(D_{cw}, m, \sigma) \quad (5)$$

Table 1 and 2 shows the fitting parameters and goodness of fit (R^2) for all observers in red/green and blue/yellow conditions. Except for Si_t, Si_1, q and z, all other parameters were fixed for R^2 did not differ empirically whether we set them free or not. The value of parameter p was set to 1 because we empirically found that fixing it at 1.00 did not affect the goodness-of-fit. Although we initially considered the input from the irrelevant dipole, shown in Figure 7 and denoted as C_{irre} in the Eq. 3, we found no significant difference in goodness of fit when we set its weighting value, Si_2, as 0. Overall our model explained 72% to 96% of the variance in the data, with rooted mean square errors (RMSE) ranging from 0.0616 to 0.1131 and mean standard error (MSE) from 0.0386 to 0.0711, across all observes and conditions.

The inverted-U curves and the shifting peak can be explained by the self-inhibitory and other-inhibitory parts in our model respectively.

doi:10.6342/NTU201600804

Table 1. List of fitting parameters and R^2 for all participants in red and green conditions.

	Observers		
	LYS	YJA	YWH
Parameters	Red (0°) [-18 dB anchor]		
p	1.00*	1.00*	1.00*
q	1.43	1.46	1.70
z	0.00	0.00	1.50
Se_t	100.00*	100.00*	100.00*
Si_t	8.54	12.60	35.84
Si_1	0.05	0.19	0.18
Si_2	0.00*	0.00*	0.00*
R^2 (%)	96.38	94.05	91.83
	Green (180°) [-18 dB anchor]		
p	1.00*	1.00*	1.00*
q	1.40	1.46	2.69
z	0.00	0.00	3.60
Se_t	100.00*	100.00*	100.00*
Si_t	10.08	12.40	143.75
Si_1	0.26	0.23	54.81
Si_2	0.00*	0.00*	0.00*
R^2 (%)	95.41	96.81	80.80
	Red (90°) [-30 dB anchor]		
p	1.00*	1.00*	
q	2.75	2.49	
z	0.29	0.00	
Se_t	100.00*	100.00*	
Si_t	1164.39	1247.45.	
Si_1	6012.37	1010.01	
Si_2	0.00*	0.00*	
R^2 (%)	82.20	71.83	
	Green (270°) [-30 dB anchor]		
p	1.00*	1.00*	
q	2.52	2.24.	
z	0.50	0.01	
Se_t	100.00*	100.00*	
Si_t	768.94	737.01.	
Si_1	450.57	1221.23	
Si_2	0.00*	0.00*	
R^2 (%)	86.09	75.95	

*Fixed parameters.

doi:10.6342/NTU201600804

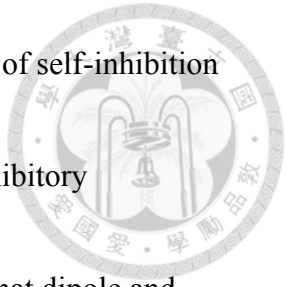

First, as the contrast value of one dipole increased, the value of self-inhibition also increased exponentially. The resulting larger contribution of inhibitory component in the denominator leads to weakened response toward that dipole and thus reduced the probability of judging the global form based on the orientation of that dipole. Second, the value of other's inhibition increased with the contrast value in other competing dipoles. Increase of competing dipole contrast led to weakened response toward the target dipole so the target dipole must gain a higher contrast level to overcome the inhibition from the competing dipole. This can explain why the peak probability shifted to the right with contrast of CCW dots.

To compare chromatic results with luminance ones, we averaged the data across two subjects and fit the mean data with our model before comparing the results of luminance condition with similar contrast range (anchor dot fixed at -30dB while CCW dot and 2 changed between -25 to -1dB) reported in Cho (2015). Results are presented in Figure 8, the fitting parameters is demonstrated in Table 3. The main difference between isoluminance and isochromatic conditions lay in the observation that the inverted-U trend was less noticeable in the former than the later.

doi:10.6342/NTU201600804

Table 2. List of fitting parameters and R^2 for all participants in blue and yellow conditions.

	Observers		
	LYS	YJA	YWH
Parameters	Blue (90°) [-7 dB anchor]		
p	1.00*	1.00*	1.00*
q	1.34	1.29	1.67
z	3.64	3.60.	0.90
Se_t	100.00*	100.00*	100.00*
Si_t	9.80.	9.44	20.14
Si_1	0.01	0.09	4.18
Si_2	0.00*	0.00*	0.00*
R^2 (%)	91.39	96.65	87.56
	Yellow (270°) [-7 dB anchor]		
p	1.00*	1.00*	1.00*
q	1.50	1.25	1.87
z	2.45	3.27	6.46
Se_t	100.00*	100.00*	100.00*
Si_t	7.61	9.72	14.25
Si_1	0.00	0.00	0.02
Si_2	0.00*	0.00*	0.00*
R^2 (%)	92.76	96.13	91.01

*Fixed parameters.

This can be explained by the inhibitory components in our divisive inhibition model. The ratio between Si_t and Si_1 (*Si* ratio) indicates the strength of self-inhibition relative to others-inhibition: the larger the ratio, the stronger the self-inhibition. Indeed, the *Si* ratios for isoluminance condition are found to be smaller than that for isochromatic condition, emphasized in bold letters in Table 3. Using *Si* ratio as the index to compare between color and luminance contrast conditions has one major benefit. That is, we were able to rule out the between-design differences between

doi:10.6342/NTU201600804

studies since we were comparing the relation between model parameters rather than directly comparing the absolute values of these parameters.

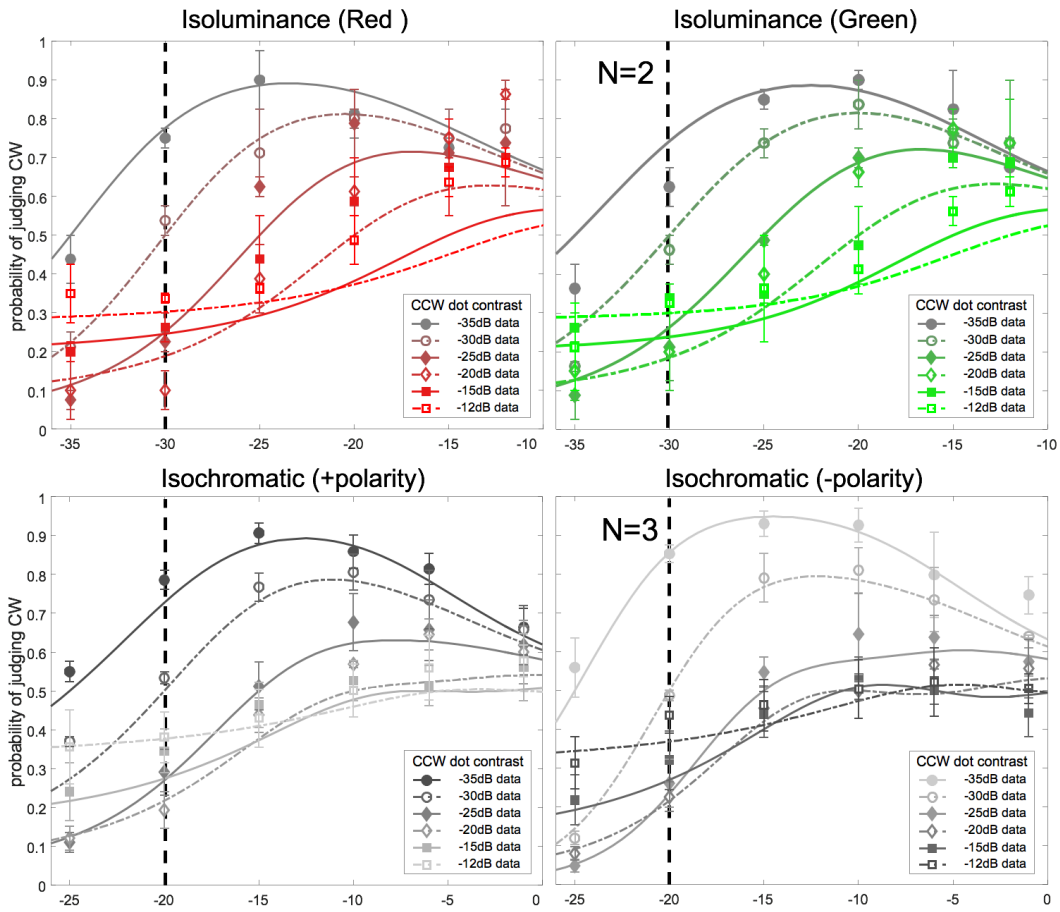

Figure 8. Average data of isoluminance (upper panel) and isochromatic (bottom panel) conditions. The filled circles demonstrate the raw data points, while the curves show the fitting results of our model. Dashed lines indicate the contrast level of the anchor dot.

Using the same model to fit averaged data of both conditions, we accounted for 82% to 97% of the variance, with rooted mean square errors (RMSE) ranging from

doi:10.6342/NTU201600804

0.0361 to 0.1005 and mean standard error (MSE) between 0.0512 and 0.0587. The fact that a divisive inhibition model reflected the observed patterns in both data suggested that a common contrast gain control mechanism was involved in both isoluminance and isochromatic conditions.

Table 3. List of fitting parameters and R^2 in isoluminance and isochromatic conditions.

	Condition	
	Isoluminance	
Parameters	Red (0°)	Green (180°)
p	1.00*	1.00*
q	2.39	2.49
z	0.00	0.18
Se_t	100.00*	100.00*
Si_t	857.87	986.72
Si_1	990.96	2822.31
Si_t/Si_1	**0.87**	**0.35**
Si_2	0.00*	0.00*
R^2 (%)	82.35	87.22
	Isochromatic	
	Positive polarity	Negative polarity
p	1.00*	1.00*
q	3.07	3.06
z	4.75	1.67
Se_t	100.00*	100.00*
Si_t	208.06	185.32
Si_1	83.12	64.37
Si_t/Si_1	**2.50**	**2.88**
Si_2	0.00*	0.00*
R^2 (%)	93.82	97.30

*Fixed parameters.

One possible limitation of our current study is that, since we used square dots as stimuli, we could not rule out luminance noise or color aberration effect completely.

doi:10.6342/NTU201600804

This leads to the possibility that our result might include luminance effect. Thus we must be cautious when comparing the difference between luminance and color contrast results. A more ideal variant of stimuli would be dots defined by Gaussian function (Chen, Wu, & Wu, 2011), which have better control over luminance noise.

Another limitation is that our model could not differentiate between pattern competition at local and global levels, since in our model, the latter one is a linear summation of all responses toward local dipoles. So the results were the same for local competition and global competition.

Future direction

To further the line of the understanding competition between coexisting grouping results, we will further examine the competition between different visual cues. We can vary intra-tripole chromaticity in the way that one of the context dots is of the same chromaticity with the anchor dot while the other is of the same color contrast and see which affects the final grouping the most. By manipulating other visual cues, such as distance between dots or disparity of dots as well as contrasts, we can determine whether it is the rule of proximity, coplanarity, or similarity of local

doi:10.6342/NTU201600804

elements that dominates the final percept.

To navigate and survive in natural environment, one needs to efficiently parsing the scene into individual meaningful objects. One way to extract correct objects out of the scene is through perceptual grouping, combining related local elements into global forms.

Evidence have shown that V4 area is involved in processing intermediate forms by integrating elementary information such as orientation from V1 and sending the combined information to higher-level regions, such as inferior temporal (IT) cortex, which is responsible for complex object processing in the hierarchy of ventral stream (Gallant et al., 1993; Gallant, Connor, Rakshit, Lewis, & Van Essen, 1996; Pasupathy & Connor, 1999).

Past researches have also demonstrated the involvement of V4 in Glass pattern or similar global form perception. In a human fMRI study, Wilkinson et al. (2000) found that concentric and radial stimuli elicited larger BOLD activation than parallel ones in V4. And Ostwald, Lam, Li, and Kourtzi (2008) demonstrated that V4 and other visual areas showed selectivity for concentric, radial and translational Glass

doi:10.6342/NTU201600804

patterns. However, V4 seems unable to differentiate clockwise from counter-clockwise spiral Glass patterns in Mannion, McDonald and Clifford's study. Combined together, these results lead to the conclusion that the form processing involving V4 does not deal with orientation information per se but global form itself. As a result, it can tell the difference between Glass patterns and random patterns but fails to distinguish spirals of opposite directions. Thus, if we present tGPs under fMRI scanning, we should also observe BOLD signals difference in V4 between tGPs with higher tendency to be judged as CW or CCW spirals (when CCW dot and CW dot contrast differs greatly) and those with chance level judging tendency (when two context dots are of same contrast).

Aside from the origin of intermediate form perception, we also want to identify which area has the potential to "differentiate" between competing Glass pattern percepts, as is presented in our tripole Glass patterns. We expect to find areas past primary visual cortex such as LOC and IT to be capable of discriminating between patterns with different contrast combination by using multivariate pattern analysis (MVPA) in our future study.

doi:10.6342/NTU201600804

doi:10.6342/NTU201600804

Conclusion

We are the first study that investigates the role of color contrast in Glass pattern perception when multiple grouping possibilities are presented simultaneously. Two significant findings were discovered in our results. First, similar to what we found in isochromatic experiments (Cho, 2015, the probability of one of the context dot grouped with the anchor dot increased with the color contrast of that context dot then decreased after a critical level, resulting in an inverted-U shape. Second, the grouping probability decreased as the contrast of the other context dot increased (in low anchor condition). Based on both isoluminance and isochromatic results, we concluded that contrast gain control mechanism was presented in both situations. However, the inhibition components differed between stimuli under luminance and chromaticity manipulation. Contribution of self-inhibition was found to be weaker than inhibition from others when we manipulated chromaticity while keeping luminance at constant level (Figure 8 and Table 3).

In the future, we can involve more visual cues such as distance between dots and disparity in our stimuli to see how these different cues interact with each other. In

doi:10.6342/NTU201600804

addition, we intend to use fMRI and other neuroimaging techniques to study which brain region might be responsible for competition of coexisting grouping results.

doi:10.6342/NTU201600804

References

Anzai, A., Peng, X., & Van Essen, D. C. (2007). Neurons in monkey visual area V2 encode combinations of orientations. *Nature neuroscience, 10*(10), 1313-1321. doi:10.1038/nn1975

Badcock, D. R., Clifford, C. W. G., & Khuu, S. K. (2005). Interactions between luminance and contrast signals in global form detection. *Vision Research, 45*(7), 881-889. doi:10.1016/j.visres.2004.09.042

Bradley, A., Switkes, E., & De Valois, K. (1988). Orientation and spatial frequency selectivity of adaptation to color and luminance gratings. *Vision Research, 28*(7), 841-856. doi:10.1016/0042-6989(88)90031-4

Cardinal, K. S., & Kiper, D. C. (2003). The detection of colored Glass patterns. *Journal of Vision, 3*(3), 2-2. doi:10.1167/3.3.2

Chen, C.-C. (2006). Local grouping in glass patterns: Chromatic and luminance tuning. *Journal of Vision, 6*(6), 759-759. doi:10.1167/6.6.759

Chen, C.-C. (2009). A masking analysis of glass pattern perception. *Journal of Vision, 9*(12), 22-22. doi:10.1167/9.12.22

doi:10.6342/NTU201600804

Chen, C.-C., Foley, J. M., & Brainard, D. H. (2000). Detection of chromoluminance patterns on chromoluminance pedestals II: model. *Vision Research, 40*(7), 789-803. doi:10.1016/S0042-6989(99)00228-X

Chen, C.-C., Wu, J.-H., & Wu, C.-C. (2011). Reduction of image complexity explains aesthetic preference for symmetry. *Symmetry, 3*(3), 443-456. doi:10.3390/sym3030443

Cho, P.-C. (2015). *Contrast Gain Control in Glass Pattern Perception.* (Masters), National Taiwan University. Available from Airiti AiritiLibrary database. (2015)

CIE. (2007). Fundamental chromaticity diagram with physiological axes - Parts 1 and 2. Technical Report 170-1. *Vienna: Central Bureau of the Commission Internationale de l' Éclairage*.

Dakin, S. C. (1997). The detection of structure in glass patterns: Psychophysics and computational models. *Vision Research, 37*(16), 2227-2246. doi:10.1016/S0042-6989(97)00038-2

Dakin, S. C., & Bex, P. J. (2001). Local and global visual grouping: Tuning for spatial

doi:10.6342/NTU201600804

frequency and contrast. *Journal of Vision, 1*(2), 4-4. doi:10.1167/1.2.4

Derrington, A. M., Krauskopf, J., & Lennie, P. (1984). Chromatic mechanisms in lateral geniculate nucleus of macaque. *The Journal of Physiology, 357*, 241-265. doi:10.1113/jphysiol.1984.sp015499

Earle, D. C. (1999). Glass Patterns: Grouping by Contrast Similarity. *Perception, 28*(11), 1373-1382. doi:10.1068/p2986

Felleman, D. J., & Van Essen, D. C. (1991). Distributed hierarchical processing in the primate cerebral cortex. *Cerebral Cortex, 1*(1), 1-47. doi:10.1093/cercor/1.1.1

Gallant, J., Braun, J., & Van Essen, D. (1993). Selectivity for polar, hyperbolic, and Cartesian gratings in macaque visual cortex. *Science, 259*(5091), 100-103. doi:10.1126/science.8418487

Gallant, J. L., Connor, C. E., Rakshit, S., Lewis, J. W., & Van Essen, D. C. (1996). Neural responses to polar, hyperbolic, and Cartesian gratings in area V4 of the macaque monkey. *Journal of neurophysiology, 76*(4), 2718-2739.

Glass, L. (1969). Moire effect from random dots. *Nature, 223*(5206), 578-580. doi:10.1038/223578a0

doi:10.6342/NTU201600804

Glass, L., & Perez, R. (1973). Perception of random dot interference patterns. *Nature, 246*(5432), 360-362. doi:10.1038/246360a0

Goodale, M. A., & Milner, A. D. (1992). Separate visual pathways for perception and action. *Trends in neurosciences, 15*(1), 20-25. doi:10.1016/0166-2236(83)90190-X

Hegdé, J., & Van Essen, D. C. (2000). Selectivity for complex shapes in primate visual area V2. *The Journal of Neuroscience, 20*(5), 61-66.

Hubel, D. H., & Wiesel, T. N. (1968). Receptive fields and functional architecture of monkey striate cortex. *The Journal of Physiology, 195*(1), 215-243. doi:10.1113/jphysiol.1968.sp008455

Ito, M., & Komatsu, H. (2004). Representation of Angles Embedded within Contour Stimuli in Area V2 of Macaque Monkeys. *The Journal of Neuroscience, 24*(13), 3313-3324. doi:10.1523/jneurosci.4364-03.2004

Johnson, E. N., Hawken, M. J., & Shapley, R. (2001). The spatial transformation of color in the primary visual cortex of the macaque monkey. *Nature neuroscience, 4*(4), 409-416. doi:10.1038/86061

doi:10.6342/NTU201600804

Kaplan, E., Shapley, R. M., & Purpura, K. (1988). Color and luminance contrast as tools for probing the primate retina. *Neuroscience Research Supplements, 8*, S151-S165. doi:10.1016/0921-8696(88)90014-X

Li, H.-H., & Chen, C.-C. (2011). Surround modulation of global form perception. *Journal of Vision, 11*(1), 17-17. doi:10.1167/11.1.17

Losada, M. A., & Mullen, K. T. (1994). The spatial tuning of chromatic mechanisms identified by simultaneous masking. *Vision Research, 34*(3), 331-341. doi:10.1016/0042-6989(94)90091-4

MacLeod, D. I., & Boynton, R. M. (1979). Chromaticity diagram showing cone excitation by stimuli of equal luminance. *Journal of the Optical Society of America, 69*(8), 1183-1186. doi:10.1364/JOSA.69.001183

Mandelli, M.-J. F., & Kiper, D. C. (2005). The local and global processing of chromatic Glass patterns. *Journal of Vision, 5*(5), 2-2. doi:10.1167/5.5.2

Mannion, D. J., McDonald, J. S., & Clifford, C. W. G. (2009). Discrimination of the local orientation structure of spiral Glass patterns early in human visual cortex. *Neuroimage, 46*(2), 511-515. doi:10.1016/j.neuroimage.2009.01.052

doi:10.6342/NTU201600804

Metzger, W., Spillmann, L. T., Lehar, S. T., Stromeyer, M. T., & Wertheimer, M. T. (2006). *Laws of seeing*: Mit Press.

Mishkin, M., Ungerleider, L. G., & Macko, K. A. (1983). Object vision and spatial vision: two cortical pathways. *Trends in neurosciences, 6*, 414-417. doi:10.1016/0166-2236(83)90190-X

Mullen, K. T. (1985). The contrast sensitivity of human colour vision to red-green and blue-yellow chromatic gratings. *The Journal of Physiology, 359*(1), 381-400. doi:10.1113/jphysiol.1985.sp015591

Ostwald, D., Lam, J. M., Li, S., & Kourtzi, Z. (2008). Neural coding of global form in the human visual cortex. *Journal of neurophysiology, 99*(5), 2456-2469. doi:10.1152/jn.01307.2007

Pasupathy, A., & Connor, C. E. (1999). Responses to Contour Features in Macaque Area V4. *Journal of neurophysiology, 82*(5), 2490-2502.

Pasupathy, A., & Connor, C. E. (2002). Population coding of shape in area V4. *Nature neuroscience, 5*(12), 1332-1338. doi:10.1038/972

Prazdny, K. (1984). On the Perception of Glass Patterns. *Perception, 13*(4), 469-478.

doi:10.6342/NTU201600804

doi:10.1068/p130469

Riesenhuber, M., & Poggio, T. (1999). Hierarchical models of object recognition in cortex. *Nature neuroscience, 2*(11), 1019-1025. doi:10.1038/14819

Stevens, K. A. (1981). The information content of texture gradients. *Biological Cybernetics, 42*(2), 95-105. doi:10.1007/bf00336727

Stockman, A., & Sharpe, L. T. (2000). The spectral sensitivities of the middle-and long-wavelength-sensitive cones derived from measurements in observers of known genotype. *Vision Research, 40*(13), 1711-1737. doi:10.1016/S0042-6989(00)00021-3

Tanaka, K. (1996). Inferotemporal cortex and object vision. *Annual review of neuroscience, 19*(1), 109-139. doi:10.1146/annurev.ne.19.030196.000545

Thorell, L. G., de Valois, R. L., & Albrecht, D. G. (1984). Spatial mapping of monkey VI cells with pure color and luminance stimuli. *Vision Research, 24*(7), 751-769. doi:10.1016/0042-6989(84)90216-5

Tobimatsu, S., Tomoda, H., & Kato, M. (1995). Parvocellular and magnocellular contributions to visual evoked potentials in humans: stimulation with

doi:10.6342/NTU201600804

chromatic and achromatic gratings and apparent motion. *Journal of the Neurological Sciences, 134*(1–2), 73-82. doi:10.1016/0022-510X(95)00222-X

Van Essen, D., Anderson, C., & Felleman, D. (1992). Information processing in the primate visual system: an integrated systems perspective. *Science, 255*(5043), 419-423. doi:10.1126/science.1734518

Wilkinson, F., James, T. W., Wilson, H. R., Gati, J. S., Menon, R. S., & Goodale, M. A. (2000). An fMRI study of the selective activation of human extrastriate form vision areas by radial and concentric gratings. *Current Biology, 10*(22), 1455-1458. doi:10.1016/S0960-9822(00)00800-9

Wilson, H. R., & Wilkinson, F. (2015). From orientations to objects: Configural processing in the ventral stream. *Journal of Vision, 15*(7), 4-4. doi:10.1167/15.7.4

Wilson, H. R., Wilkinson, F., & Asaad, W. (1997). Concentric orientation summation in human form vision. *Vision Research, 37*(17), 2325-2330. doi:10.1016/S0042-6989(97)00104-1

Wilson, J. A., & Switkes, E. (2005). Integration of differing chromaticities in early

doi:10.6342/NTU201600804

and midlevel spatial vision. *Journal of the Optical Society of America A, 22*(10), 2169-2181. doi:10.1364/JOSAA.22.002169

Wilson, J. A., Switkes, E., & De Valois, R. L. (2004). Glass pattern studies of local and global processing of contrast variations. *Vision Research, 44*(22), 2629-2641. doi:10.1016/j.visres.2003.06.001

doi:10.6342/NTU201600804

doi:10.6342/NTU201600804

Appendix

Threshold session

We measured the threshold of observer LYS. In the threshold measurement session, the procedure was the same as in experiment sessions except for that only one of the context dots was presented with the anchor dot in each stimulus and that the two dots were always with the same contrast level. We manipulated the contrast ranges between -40dB to -28dB for red and green, -19dB to -7dB for blue and yellow. The threshold was defined as the 75% correct response of the observer judging the stimulus as CW or CCW spiral by fitting a cumulative normal psychometric function to the data. The measured thresholds were -33.90 dB for red (0°), -33.09 dB for green (180°), -13.98 dB for blue (90°), and -14.77 dB for yellow (270°).

doi:10.6342/NTU201600804